

# Enhancement of Critical Current Density of Yttrium Barium Copper Oxide Thin Films by Introducing Nano dimensional Cerium Oxide Defects

Tochukwu Emeakaroha<sup>1</sup>, Floyd James<sup>1</sup> & Abebe Kebede<sup>1</sup>

<sup>1</sup> Department of Physics and Astronomy North Carolina Agricultural and Technical State University, Greensboro, North Carolina, 27401, USA

Correspondence: Tochukwu Emeakaroha, Department of Physics and Astronomy North Carolina Agricultural and Technical State University, Greensboro, North Carolina, 27401, USA. E-mail: tmemeaka@aggies.ncat.edu

Received: October 14, 2018

Accepted: November 2, 2018

Online Published: November 30, 2018

doi:10.5539/apr.v10n6p109

URL: <https://doi.org/10.5539/apr.v10n6p109>

## Abstract

The critical current density,  $J_c$  has been the most important parameter used in the design and engineering of effective devices which is one of the implementation of high temperature superconductors (HTSC). In this work, an effort has been made to further improve the critical current density of  $\text{YBa}_2\text{Cu}_3\text{O}_{7-x}$  (YBCO) thin films by preventing the magnetic flux line lattice against the Lorentz force by pinning it in place with the aid of nano-dimensional defects. These defects were generated by distributing nano sized  $\text{CeO}_2$  islands after YBCO layer was created on  $\text{LaAlO}_3$  substrates perpendicular to the film using pulsed laser deposition (PLD) technique. Three samples with buffer layers of  $\text{CeO}_2$  were prepared.  $\text{CeO}_2$  with 50 pulses, 100 pulses and 150 pulses, after each 1000 pulses of YBCO were prepared five layers for each of the samples. The structural characterization of YBCO/ $\text{CeO}_2$  and YBCO pristine films were carried out using x-ray diffraction (XRD) and scanning electron microscopy (SEM). Superconducting properties were measured using a vibrating sample magnetometer (VSM).  $J_c$  for the pure YBCO and the YBCO/ $\text{CeO}_2$  films were calculated from magnetization (M) versus Field (H) loops using Bean's model.  $J_c$  for the 50 pulses of YBCO/ $\text{CeO}_2$  films was found to be increased slightly by an order of magnitude of about 40% with respect to those of YBCO films without the nano dimensional defects.

**Keywords:** high temperature superconductivity, thin films, YBCO,  $\text{CeO}_2$ , critical current density.

## 1. Introduction.

$\text{YBa}_2\text{Cu}_3\text{O}_{7-x}$  (YBCO) film has attracted a lot of attention in electrical power applications due to its high critical transition temperature  $T_c$  ( $>90$  K) and critical current density  $J_c$  ( $>1$  MA  $\text{cm}^{-2}$ ) (Lei, Zhao, Xu, Wu, & Chen, 2011; Haugan, Barnes, Brunke, Manrtense & Murphy, 2003). The growth of  $\text{YBa}_2\text{Cu}_3\text{O}_{7-x}$  (YBCO) thin films is of great interest for superconducting applications because of its power transmission magnetic shielding, low phase noise oscillators, magnetic resonance imaging receiver coils (Chen et al., 2016; Matsuunotoet al., 2004; Rejith, Vidya & Thomas, 2015; Zhao, Ito & Goto, 2014). Fine precipitates, dislocations, grain boundaries and vacancies are many kinds of crystalline defects, being considered as pinning centers (Zhao, Ito & Goto, 2014; Kujur, Sahoo, Panda, Asokan & Behera, 2013). The pinning centers depend on size, shape and concentration to achieve effective defects. The critical current density is highly influenced by flux lattice motion due to thermal fluctuations and Lorentz force due to applied magnetic fields. To maintain the necessary levels of high  $J_c$  in high applied magnetic fields we need high spatial densities or naturally occurring growth defect to suppress the thermal fluctuations to stop the vortex mobility by pinning them. Although nanodots of  $\text{CeO}_2$  have been shown to induce additional flux pinning, this has always been due to strain in the YBCO lattice because of these inclusions. Such strain however, could have detrimental effect on the YBCO. Aside from the thickness dependence of  $J_c$ , there is also a limitation placed on the thickness at which such films could be grown (Uzun & Avci, 2014; Zhao, Iton & Goto, 2014; Sueyoshi, Kotaki, Fujiyoshi, Mitsugi, Ikegami & Ishikawa, 2013).

(Huang, Li, Wang, Qi, Sebastain, Haugan, & Wang, 2017), reported the enhanced flux pinning properties of YBCO thin films with various pinning landscapes a magnetic nanocomposite of  $\text{La}_{0.7}\text{Sr}_{0.3}\text{MnO}_3$  (LSMO) $_x$  ( $\text{CeO}_2$ ) $_{1-x}$  was incorporated into YBCO as either a cap layer or a buffer layer but the defect pinning and magnetic pinning are introduced in the systems giving the  $J_c$  at 77K to be around 4.66MA/ $\text{cm}^2$  (Xu et al., 2012), reported the influence

of CeO<sub>2</sub>-cap layer on the texture and critical current density of YBCO film, here the found that the texture and J<sub>c</sub> of YBCO film were largely dependent on the texture of CeO<sub>2</sub>-cap layers under optimized deposition conditions, with the increase of the degree of in-plane and out-plane texture of CeO<sub>2</sub>-cap layers, there was a decrease in the J<sub>c</sub> of the YBCO thin films from 4.23MA/cm<sup>2</sup> to 0.47MA/cm<sup>2</sup>. (Lee, Kim, Park & Park, 1996), agreed that addition of CeO<sub>2</sub> into YBCO will increase the critical current density to an extent at 77K, they reported 2x 10<sup>4</sup>A/cm<sup>2</sup> an increased by lowering the measuring temperature. (Solovyov, Bagarinao, Li, Si, Win, Zhou, Wiesmann & Qing, 2010), used active (001) Ceria (CeO<sub>2</sub>) buffer to modify the structure of the epitaxial high temperature superconductor YBCO which resulted with 0.8μm thick film exhibiting strong enhancement of the critical current density of 4.2MA/cm<sup>2</sup>. (Feng et al., 2015), used CeO<sub>2</sub> cap layers for high temperature superconducting, were YBCO films were epitaxially deposited on the as-growth CeO<sub>2</sub>/ YSZ (001) stack using water- free metal organic deposition (MOD) method to obtain 1.92MA/cm<sup>2</sup> as J<sub>c</sub> at 77K at 0.5Pa deposition pressure.

Pulsed laser deposition (PLD) which is one of the physical deposition methods has been a promising technique for thin film growth and for fabricating nano-dimensional/nano-dots within epitaxial, textured or polycrystalline thin film matrices in recent years (Bhaumik et al., 2017; Haque, Pant and Narayan, 2018; Haque and Narayan, 2018; Karnati, Haque, Taufique and Ghosh, 2018). In the present study, we have generated the nanostructures on LaAlO<sub>3</sub> substrates by depositing YBCO and YBCO/CeO<sub>2</sub> multilayer thin films. To investigate the effects of introducing nano dimensional CeO<sub>2</sub> defects on (current density) J<sub>c</sub> and the micro structure of YBCO.

## 2. Experimental Procedure

Several alternating layers of YBCO/CeO<sub>2</sub> thin films were grown on single crystal LaAlO<sub>3</sub> substrates using pulsed laser deposition technique. YBCO target of 99.9% with density of 5g/cm<sup>3</sup> and 99.9% of CeO<sub>2</sub> target, both were ordered from MTI corporation were used for this experiment. The substrate which is LaAlO<sub>3</sub> with orientation (100) and size of (10 × 10) and (5 × 5)mm were used for the deposition, cleaned with acetone, methanol, and ethanol for 10 mins each, under ultrasonic to remove dirt and oil, after that the substrate was dropped inside hydrogen fluoride to also remove oil particle if there is any left and then dry. The deposition chamber was cleaned with acetone and methanol to remove dirt particle inside it. We then mounted the cleaned substrate on the holder with silver paste. Ablation was performed using KrF laser source of a wavelength 248nm. The ablation was done at (300) mJ of laser energy with a repetition of 5Hz. The aperture size was 12 x 4 mm<sup>2</sup> and laser spot size was 1 x 4 mm<sup>2</sup>. The target-substrate distance was maintained at 4cm. A based pressure of 10<sup>-7</sup> Torr was maintained before the deposition; the deposited films were cooled down naturally in 600 mTorr of oxygen gas. To determine the optimum oxygen pressure for YBCO depositions, experiments were carried out at oxygen pressures of 400 mTorr. For this study three samples were chosen based on their yield and structural quality. They are identified as 50 Pulses, 100 Pulses and 150 Pulses samples based on the number of laser pulses used for a layer of CeO<sub>2</sub>. The films were deposited on LaAlO<sub>3</sub> single crystal substrates with (001) direction. Starting with YBCO followed by CeO<sub>2</sub>, 10 layers of films were deposited for each sample tabulated below.

Table 1. The multilayer deposition showing all the samples

LAYER	Sample 1: 50 Pulses	Sample 2: 100 Pulses	Sample 3: 150 Pulses
YBCO	1000 Pulses	1000 Pulses	1000 Pulses
CeO <sub>2</sub>	50 Pulses	100 Pulses	150 Pulses
YBCO	1000 Pulses	1000 Pulses	1000 Pulses
CeO <sub>2</sub>	50 Pulses	100 Pulses	150 Pulses
YBCO	1000 Pulses	1000 Pulses	1000 Pulses
CeO <sub>2</sub>	50 Pulses	100 Pulses	150 Pulses
YBCO	1000 Pulses	1000 Pulses	1000 Pulses
CeO <sub>2</sub>	50 Pulses	100 Pulses	150 Pulses
YBCO	1000 Pulses	1000 Pulses	1000 Pulses
CeO <sub>2</sub>	50 Pulses	100 Pulses	150 Pulses

### 2.1 Multilayer Deposition of YBCO/CeO<sub>2</sub>

The 50 Pulses sample contains five layers of YBCO and 5 layers of CeO<sub>2</sub>. The difference between the three samples is differences in the thickness of the CeO<sub>2</sub> layers. Single and multilayer samples were prepared using pulsed laser deposition. Also, a fourth sample of pure YBCO with 5000 pulses was made to be used for comparison of vital data such as the superconducting transition temperature and critical current density. The

experimental conditions for deposition of pure YBCO films are: Deposition temperature of 800°C, 825°C, 850°C, after several depositions we settled at 850°C for our optimum deposition temperature, an oxygen pressure of 400 mTorr, laser energy of 300 mJ, and laser pulse repetition rate of 5Hz. The pure YBCO films were cooled under an oxygen pressure of 600mTorr. The deposition parameters for CeO<sub>2</sub> nano dimensional were same for the pure YBCO in terms of the deposition temperature.

X-ray diffraction (XRD) and Scanning Electron Microscopy (SEM) were carried out to investigate the film microstructures and to calculate/measure oxygen deficiency in the samples. The superconducting properties of all the samples were measured using physical property measurement system (PPMS), it has an option called vibrating sample magnetometer (VSM) where the sample was attached to and then inserted inside the PPMS. Magnetization (M) Vs Temperature (T) in low field of 5 Oe were carried out to determine the critical temperature for each of the samples. (Haywoods, Oh, Kebede, Pai, Sankar, Christen, Pennycok & Kumar, 2008). The magnetic field dependence of the critical current density J<sub>c</sub> (H) was calculated using bean model from the magnetization versus field of the hysteresis loop (M-H) for several fixed temperatures.

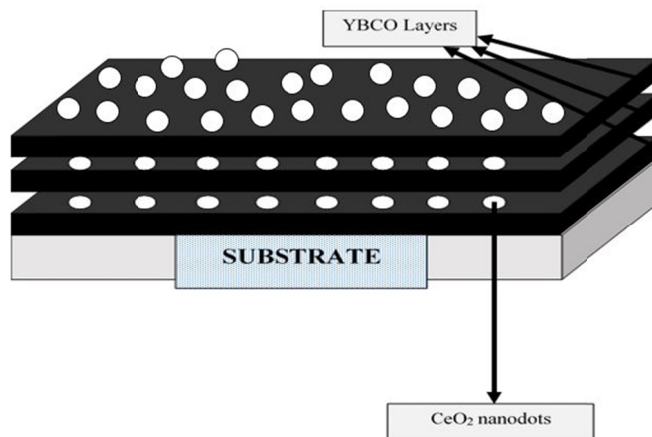


Figure 1. Schematic diagram of multilayer deposition of YBCO/CeO<sub>2</sub>. 1000 pulses of YBCO was first deposited on the first layer of the substrate followed by CeO<sub>2</sub> which was varied (50,100,150) Pulses. These layers were done five times ending it with CeO<sub>2</sub>

### 3. Results and Discussion

X-ray diffractometer was performed on all the films to determine film crystallinity and specially to analyze the non-superconducting impurity diffraction peaks. A high quality epitaxial YBCO film has been observed.

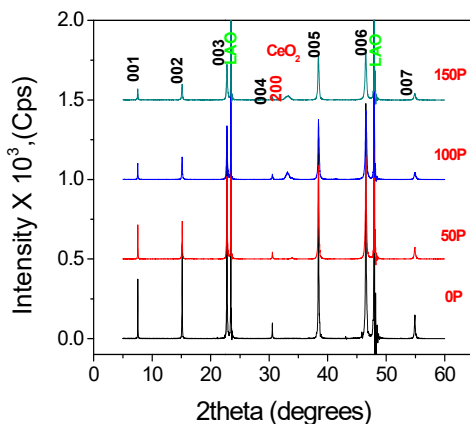


Figure 2. XRD pattern of Pure YBCO and YBCO/CeO<sub>2</sub> where 0P is for the pure YBCO and 50P,100P and 150P are for the YBCO/CeO<sub>2</sub>

The (00l) peaks in the XRD-spectra indicate that YBCO thin films are highly c-axis oriented, which is commonly observed and corresponds to the natural growth of the material. The XRD pattern from the YBCO and YBCO/CeO<sub>2</sub> deposited on LaAlO<sub>3</sub> at 850°C and 300mTorr of oxygen pressure, is shown in figure 2. From the graph above we can observe that (00l) peaks are (001) at 7.56°, (002) at 15.18°, (003) at 23.7°, (004) at 31.2°, (005) at 38.5°, (006) at 47°. The peaks of the substrate were also observed with corresponding degrees at 23.5° and 48.3°. All the samples of YBCO and YBCO/CeO<sub>2</sub> was highly c-axis oriented with good sharp and strong peaks. The CeO<sub>2</sub> appears in the graph below as an independent phase. The peak of CeO<sub>2</sub> are observed only at 32.8° (200) orientation from the graph we can observe that the intensity increases as the number of pulses are added. The XRD pattern for the 50P YBCO/CeO<sub>2</sub> was not resolvable, probably due to the small amount of the CeO<sub>2</sub> size and low density. The presence of (00l) confirmed that the deposition parameters used for this work were good and suitable for the growth of YBCO on LAO substrates. No second phase such as Y<sub>2</sub>Cu<sub>2</sub>O and CuO were found in this case. Only YBCO and CeO<sub>2</sub> phase was formed with a high intensity. From the XRD the oxygen deficiency was calculated for the samples using equation 1 (Coll, Gazque, Huhne, Holzapfel, Morilla, Lopez, Pomar, Sandimenge, Puig & Obradors, 2009), and the results are shown on Table 2.

Oxygen deficiency calculated from c-axis

$$c = 12.736 - 0.1501(7 - x)$$

Or

$$x = \left( \frac{c - 11.6853}{0.1501} \right) \tag{1}$$

Table 2. Oxygen deficiency calculated from c-axis

Sample Name	c- axis pattern (°)	Oxygen deficiency(°)
Sample I (800°C)	11.7056	0.148
Sample II (825°C)	11.7053	0.133
Sample III (850°C)	11.7003	0.099
Sample IV (50Pulses)	11.6978	0.083
Sample V (100Pulses)	11.6958	0.063
Sample VI (150Pulses)	11.6901	0.031

The scanning electron microscopy (SEM) was performed on the samples, it revealed the surface morphologies of thin films. Figure 3 (a and b) shows the SEM image of pure YBCO and 50 pulses of YBCO/CeO<sub>2</sub>. Figure 3 (c and d) shows the SEM of the YBCO/CeO<sub>2</sub> samples for (100 and 150) pulses respectively with nano dimensional defects, the pure YBCO reveals that they YBCO are well packed with long and extended grains randomly oriented in all direction with sizes vary from 1-5µm.

$$D = \frac{0.9\lambda}{\beta \cos\theta} \tag{2}$$

Where,

D = Grain size,

λ = Wavelength of X-ray used,

β = Full width at half maxima of the peak (FWHM) in radians,

θ = Bragg's angle

Table3. Calculated Crystalline size of CeO<sub>2</sub>

Sample name	Peak Width	2theta	Theta	Wavelength	Grain Size
50 pulses	NIL	NIL	NIL	1.5406nm	NIL
100 pulses	0.881°	33.29°	16.64°	1.5406nm	1.64nm
150 pulses	0.587°	33.12°	16.56°	1.5406nm	2.46nm

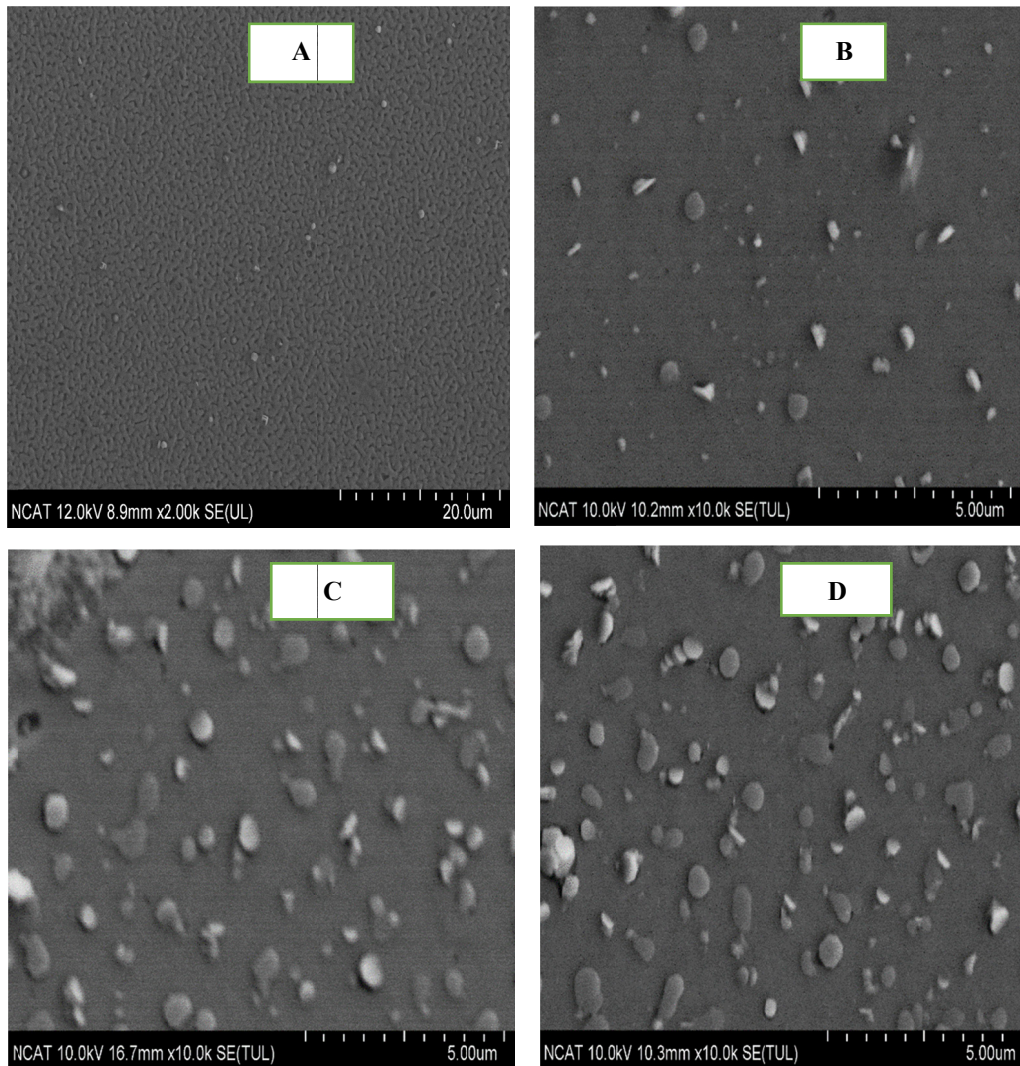


Figure 3. SEM images showing the microstructure of the samples, (A) Pure YBCO, (B) 50pulses, (C)100pulses, (D) 150pulses of YBCO/CeO<sub>2</sub>

To measure and confirm the critical temperature ( $T_c$ ) of HTSC samples, zero field cooled magnetization measurement was performed using the Vibrating Sample Magnetometer (VSM) option on the PPMS. For these measurements, the sizes of the samples both the pure YBCO and the multilayer YBCO and CeO<sub>2</sub> were reduced to (2 x 2) mm<sup>2</sup> by cutting it with a diamond cutter. The samples were mounted in such a way that the magnetic field was parallel to the c-axis, that is, the magnetic field was perpendicular to the film surface. After mounting the sample on the holder, the PPMS system was cooled down to 10K. As can be seen in figure 4 the magnetization versus temperature measurement was carried out for all the samples. The results of the measurements are summarized in Table 3 below. The transition to the superconducting phase was sharp for more samples, and the  $T_c$  in the range of 89 K to 92 K was obtained and this agrees with some of the literature (Kumar, Apte, Pinto, Sharon & Gupta, 1994; Haruta et al., 2013; Bobylev, Gerasimov & Zyuzeva, 2015; Pahike et al., 2016; Liu, Song, Wang & Zhang, 2016; Zhai et al., 2015). It was also observed that the deposition temperature of 800°C has given a larger volume fraction of superconductivity than the other two deposition temperatures and it is about twice the fraction than for the 850°C. In this case the factors influencing the volume fraction may include inconsistency in controlling the growth parameter. This experiment shows the effect of different pulses of CeO<sub>2</sub> on the transition temperature and the superconducting volume fraction. As can be seen the superconducting volume fraction is highest for the 150 Pulses compared with the 100 Pulses and 50 Pulses. On the other hand, the 50 Pulses sample gave the highest  $T_c$ . This is because the number of CeO<sub>2</sub> was small compared to others.

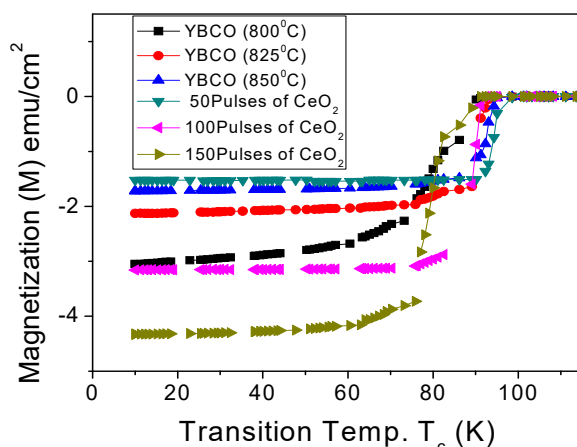


Figure 4. Magnetization Versus Transition Temperature (K) of all the sample, pure YBCO at different deposition temperature and (50, 100, 150) pulses of YBCO/CeO<sub>2</sub> at the same deposition temperature

Table 4. List of samples details and their superconducting properties

Sample Name	Deposition Temperature °C	Oxygen pressure (m Torr)	Laser Energy(mJ)	T <sub>c</sub> (K)
Sample I (YBCO)	800	400	300	87.2
Sample II (YBCO)	825	400	300	89.0
Sample III (YBCO)	850	400	300	91.1
Sample IV YBCO/CeO <sub>2</sub> (50Pulses)	850	400	300	92.0
Sample V YBCO/CeO <sub>2</sub> (100Pulses)	850	400	300	91.0
Sample VI YBCO/CeO <sub>2</sub> (150Pulses)	850	400	300	87

Figure 5 shows T<sub>c</sub> as a function of number of pulses for the onset transition temperature. From the plot, we can deduce that the T<sub>c</sub> was high for Pure YBCO (0 pulses) and after the introduction of 50 pulses of CeO<sub>2</sub> the T<sub>c</sub> increased slightly. Similar changes were observed at 100 pulses and 150 pulses the T<sub>c</sub> decreases as the number of pulses were added. This is a clear indication that the CeO<sub>2</sub> defects were randomly introduced into superconducting matrix. Figure 6 shows that the obtained magnetic moment is in the emu units, which was converted to magnetization (emu/cm<sup>3</sup>) by dividing the magnetic moment by the volume of the sample. The area of the thin film sample was (2 x 2) mm<sup>2</sup>. The thickness of the film was maintained at 100nm for pure YBCO.

The magnetic moment was obtained for the field swept from desired positive field to zero field and zero field to desired positive field. The value of the current density depends on several parameters including deposition temperature (T<sub>D</sub>), the number of pulses (P), external magnetic field (H) and the temperature at which it is measured (T). i.e J<sub>c</sub> = (T<sub>D</sub>, P, H, T). (T<sub>D</sub> and P) are sample parameters that can be controlled during the sample growth. Keeping these two parameters fixed, J<sub>c</sub> depends on H and T. The most determining sample condition for the value of J<sub>c</sub> are the flux pinning centers introduced by the CeO<sub>2</sub> nano dots and randomly distributed in the superconducting matrix, the pinned flux experiences forces because thermal fluctuations and the Lorentz force that lead to flux lattice melting. Using Bean’s formula, critical current density (J<sub>c</sub>), was calculated for pure YBCO and multilayer CeO<sub>2</sub> nano dimensional defect. Bean’s formula is given as (Matsuunoto, Horide, Osamura, Mukaida, Yoshida, Ichinose & Horii, 2004; Rejith, Vidya & Thomas, 2015; Zhao, Ito & Goto, 2014)

$$J_c = 30 \Delta M/a \tag{3}$$

where ΔM is the difference of magnetization at a field, in emu/cm<sup>3</sup>, a is the area of the inscribed circle, in cm and J<sub>c</sub> is critical density in A/cm<sup>2</sup>.

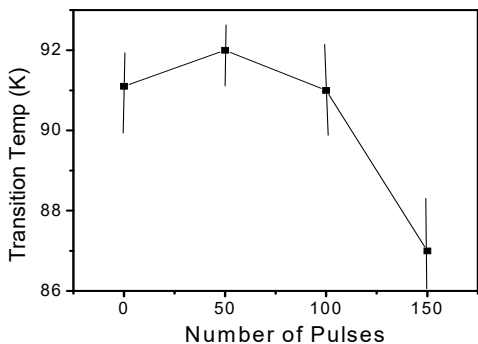


Figure 5. Transition Temperature Versus Number of pulses of all the samples, Pure YBCO and (50,100,150) Pulses of YBCO/CeO<sub>2</sub>

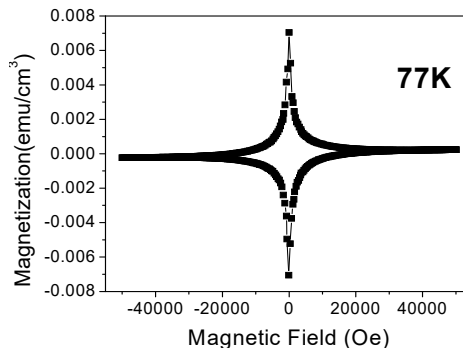


Figure 6. Magnetization Vs Magnetic field (hysteresis loop at 77K of 50 pulses)

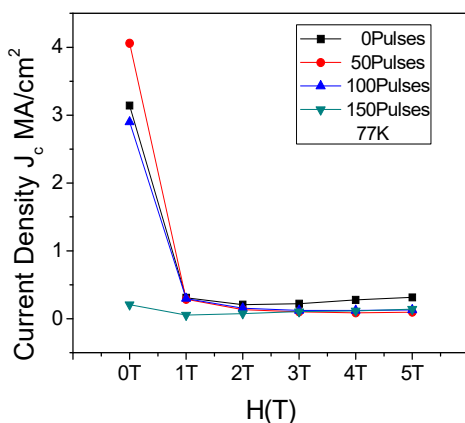


Figure 7. Current Density Versus Magnetic Field H(T) for Pure YBCO and (50,100,150) Pulses of YBCO/CeO<sub>2</sub>

Figure 8 shows the plots of the current density  $J_c$  against the field in Tesla, at 77K it explains that the 50 pulses of the YBCO/CeO<sub>2</sub> in the multilayer gave highest  $J_c$  which was about 4.1 MA/cm<sup>2</sup> this agrees with other report (Huang, Li, Wang, Qi, Sebastain, Haugan & Wang, 2017; Xu, Liu, Wang, Zhu, Zhu & Li, 2012; Lee, Kim, Park & Park, 1996; Feng, Zhang, Qu, Huang, Xiao, Zhu, Lu, Shi, & Han, 2015) against the pure YBCO and we observed that the more CeO<sub>2</sub> was added in the multilayer the less the  $J_c$ , and  $T_c$  we got, and this did not affect its structural properties. Table 5 below shows some current density of other literature which agree with our result. (Zhu, Wei, Yan, Tei, Jing, Liang, Bin, He & Wei, 2016). Figure 8 shows critical current density  $J_c$  as a function of measured temperature of all the samples.

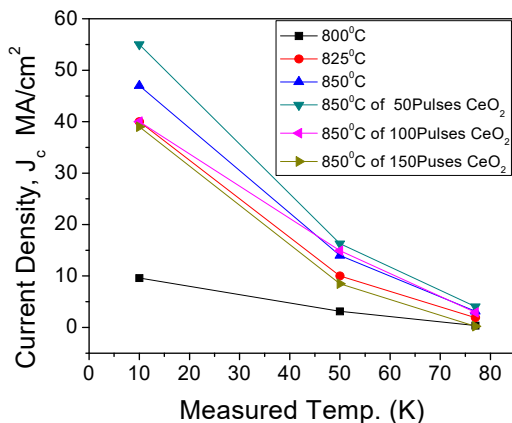


Figure 8. Current density Versus Measured Temperature (K) of all the samples at 10K, 50 K and 77K

Table 5. Comparing the current density with other literatures

Literatures	Current Density at 77K
Huang et al. (2017)	4.66MA/cm <sup>2</sup>
Xu et al. (2012)	4.23MA/cm <sup>2</sup>
Lee et al. (1996)	2x10 <sup>4</sup> A/cm <sup>2</sup>
Solovyov et al. (2010)	4.2MA/cm <sup>2</sup>

#### 4. Conclusion

In conclusion, we conclude that enhancing flux pinning in superconductors is central to improving their current carrying capability ( $J_c$ ) and their ability to be used in magnetic fields but in this study only on 50 pulses that the  $J_c$  increases slightly, Unlike other superconducting parameters, such as critical Temperature ( $T_c$ ) and critical magnetic field.  $J_c$  is not intrinsically limited to the material of system. In this work, the micro structure and critical current density of  $YBa_2Cu_3O_{7-\delta}$  films have been found to improve very slightly with the introduction of nano dimensional multilayer  $CeO_2$ . Evidence from magnetic properties and XRD, shows that no second phase such as  $Y_2Cu_2O$  and  $CuO$  were found. Only YBCO and  $CeO_2$  phase were formed with a high intensity, while SEM shows that pure YBCO has long and extended grain randomly oriented in all direction with size vary from 1-5 $\mu$ m with the grain very closely packed to each other. TEM analysis and X-ray diffraction texture analysis of  $CeO_2$  layers will be incorporated in the future work.

#### References

- Bhaumik, A., Haque A., Taufique M.F.N., Karnati, P., Patel, R., & Ghosh, K. (2017). Reduced graphene oxide thin films with very large charge carrier mobility using pulsed laser deposition. *J Material Sci Eng.*, 6(4), 364. <https://doi.org/10.4172/2169-0022.1000364>.
- Bobylev, I. B., Gerasimov, E.G., & Zyuzeva N. A. (2015). Improvement of critical parameters of  $YBa_2Cu_3O_{6.9}$  by low temperature treatment in the presence of water vapors. *Cryogenics*, 72, 36. <https://doi.org/10.1016/j.cryogenics.2015.08.003>
- Chen, Y., Bian, W., Huang, W., Tang, X., Zhao, G., Li, L., Li, N., Huo, W., Jia, J., & You, C. (2016). High Critical Current Density of  $YBa_2Cu_3O_{7-x}$  Superconducting Films Prepared through a DUV-assisted Solution Deposition Process, *Scientific Reports.*, 6, 38257. <https://doi.org/10.1038/srep38257>.
- Coll, M., Gàzquez, J., Huhne, R., Holzapfel, B., Morilla, Y., García-López, J., ... Obradors, X. (2009). All chemical  $YBa_2Cu_3O_7$  superconducting multilayers: Critical role of  $CeO_2$  cap layer flatness. *J. Material. Research*, 24, 1446. <https://doi.org/10.1557/jmr.2006.0269>.
- Feng, F., Zhang, Y., Qu, T., Huang, R., Xiao, S., Zhu, Y., Lu, H., Shi, K., & Han Z. (2015). Surface characterization of as-grown  $CeO_2$  cap layer morphology evolution and critical current density of post-deposited YBCO films. *Materials Express*, 5, 534. <https://doi.org/10.1166/mex.2015.1265>.
- Haque, A., & Narayan, J. (2018) Electron field emission from Q-carbon” *Diam. Relat. Mater.*, 86, 71- 78. <https://doi.org/10.1016/j.diamond.2018.04.008>.
- Haque, A., Pant, P., & Narayan, J. (2018). Large-area diamond thin film on Q-carbon coated crystalline sapphire by HFCVD” *Journal of crystal growth*, 504, 17-25. <https://doi.org/10.1016/j.jcrysgro.2018.09.036>
- Haruta, M., Saura, K., Fujita, N., Ogura, Y., Khinose, A., Maeda, T., & Horii S. (2013). Relationship between vortex pinning properties and microstructure in Ba-Nb-O-doped  $YBa_2Cu_3O_y$  films. *Physica C Superconductivity and its Applications*, 494, 158.
- Haugan, T., Barnes, P.N., Brunke, L., Manrtense, I., & Murphy J. (2003). Effect of deposition temperature on the orientation and electrical properties of  $YBa_2Cu_3O_{7-\delta}$  films prepared by laser CVD using liquid-source evaporation, *Physica C*, 397, 47.
- Haywoods, T., Oh, S. H., Kebede, A., Pai, D. M., Sankar, J., Christen, D. K., Pennycook, S. J., & Kumar, D. (2008). *Physica C Superconductivity and its Applications*, 468, 2313. <https://doi.org/10.1016/j.physc.2008.07.008>
- Huang, J., Li, L., Wang, X., Qi, Z., Sebastian, M., Haugan, T. J., & Wang H. (2017). Enhanced flux pinning properties of YBCO thin films with various pinning landscapes. *IEEE transactions on applied superconductivity*, 27, 4.

- Karnati, P., Haque, A., Taufique, M.F.N., & Ghosh, K. (2018). A systematic study on the structural and optical properties of vertically aligned zinc oxide nanorods grown by high pressure assisted pulsed laser deposition technique” *Nanomaterials*, 8(2), 62. <https://doi.org/10.3390/nano8020062>
- Kujur, A., Sahoo, M., Panda, R. K., Asokan, K., & Behera D. (2013). The effect of 200 MeV swift heavy Ag ions on the transport property of  $\text{YBa}_2\text{Cu}_3\text{O}_{7-\delta}$  thick films. *Physica C. Superconductivity and its Applications*, 492, 168. DOI 10.1007/s10948-014-2486-3.
- Kumar, D., Apte, P.R., Pinto, R., Sharon, M., & Gupta L. C. (1994). Aging effects and passivation studies on undoped and Ag-doped  $\text{YBa}_2\text{Cu}_3\text{O}_{7-x}$  laser-ablated thin-film. *J. Electrochemical. Society*, 141, 611.
- Lee, K. W., Kim, C. J., Park, Y. K., & Park, J. C. (1996). Critical Current Density and Irreversibility Line in Melt-Textured YBCO with  $\text{CeO}_2$  Addition. *Chinese Journal of Physics*, 34, 2.
- Lei, L., Zhao, G., Xu, H., Wu, N., & Chen, Y. (2011). Influences of  $\text{Y}_2\text{O}_3$  nanoparticle additions on the microstructure and superconductivity of YBCO films derived from low-fluorine solution, *Material Chemistry and Physics*, 127, 91. <https://doi.org/10.1016/j.matchemphys.2011.01.030>
- Liu, J., Song, S., Wang, Q., & Zhang, Q., (2016). Critical Current Analysis of an YBCO Insert for Ultrahigh-Field All-Superconducting Magnet. *IEEE transactions on applied superconductivity*, 26, 3.
- Matsuunoto, K., Horide, T., Osamura, K., Mukaida, M., Yoshida, Y., Ichinose, A., & Horii. S. (2004). Enhancement of critical current density of YBCO films by introduction of artificial pinning centers due to the distributed nano-scaled  $\text{Y}_2\text{O}_3$  islands on substrate. *Physica C. Superconductivity and its Applications*, 412-414, 1267. <https://doi.org/10.1016/j.physc.2004.01.157>
- Pahlke, P., Sieger, M., Chekhonin P., Skrotzki, W., Hänisch, J., Usoskin, A., Strömer, J., Schultz, L., & Hühne, R. (2016). Local Orientation Variations in YBCO Films on Technical Substrates a Combined SEM and EBSD Study. *IEEE transactions on applied superconductivity*, 26, 3.
- Rejith, P.P., Vidya, S., & Thomas, J. K. (2015). Influence of  $\text{YBa}_2\text{HfO}_{5.5}$  – derived secondary phase on the critical current density and Flux-Pinning force of  $\text{YBa}_2\text{Cu}_3\text{O}_{7-\delta}$  thick films. *Materials Science and Engineering*, 73, 012146. <https://doi.org/10.1088/1757-899X/73/1/012146>
- Solovyov, V.F., Develos-Bagarinao, K., Li, Q., Si, W. D., Win, L. J., Zhou, J., Wiesmann H., & Qing, J. (2010). Strong pinning in thick  $\text{YBa}_2\text{Cu}_3\text{O}_7$  layers mediated by catalysis of a new long- period metastable cuprate phase. *Journal of Applied Physics*, 108, 113912. <https://doi.org/10.1063/1.3517467>
- Sueyoshi, T., Kotaki, T., Fujiyoshi, T., Mitsugi, F., Ikegami, T., & Ishikawa, N. (2013). Angular dependence of critical current density and n-values in  $\text{BaZrO}_3/\text{YBa}_2\text{Cu}_3\text{O}_y$  quasi-multilayered films with columnar defects. *Physica C Superconductivity and its Applications*, 494, 153.
- Uzun, Y., & Avci, I. (2014). Magnetic shielding performance of superconducting YBCO thin film in a multilayer device structure. *Physica C Superconductivity and its Applications*, 507, 90.
- Xu, D., Liu, L., Wang, Y., Zhu, S., Zhu, P., & Li, Y. (2012). Influence of  $\text{CeO}_2$ -Cap Layer on the Texture and Critical Current Density of YBCO Film. *J. Superconductor Nov. Magnetism*, 25, 197. <https://doi.org/10.1007/s10948-011-1251-0>
- Ye S., Suo H., Wu Z., Liu M., Xu Y., Ma L., & Zhou M. (2011). Preparation of solution-based YBCO Films with  $\text{BaSnO}_3$  particle. *Physica C Superconductivity and its Applications*, 47, 265.
- Zhai, W., Shi, Y., Durrell, J. H., Dennis, A. R., Zhang, Z., & Cardwell, D. A. (2015). The Influence of Y-211 Content on the Growth Rate and Y-211 Distribution in Y–Ba–Cu–O Single Grains Fabricated by Top Seeded Melt Growth. *Crystal Growth & Design*, 15, 907. <https://doi.org/10.1021/cg501135q>
- Zhao, P., Ito, A., & Goto, T (2014). Orientation control and electrical properties of  $\text{YBa}_2\text{Cu}_3\text{O}_{7-\delta}$  deposited onto  $\text{CeO}_2$  buffer films by laser chemical vapor deposition using liquid source precursors. *Thin Solid Films*, 564, 92. <https://doi.org/10.1016/j.tsf.2014.05.040>
- Zhao, P., Ito, A., & Goto, T. (2014). Effect of deposition temperature on the orientation and electrical properties of  $\text{YBa}_2\text{Cu}_3\text{O}_{7-\delta}$  films prepared by laser CVD using liquid-source evaporation, *Ceramics International*, 40, 2057. <https://doi.org/10.1016/j.ceramint.2013.07.118>
- Zhu, D. F., Wei, G.H., Yan, W. H., Tei, Q., Jing, S.H., Liang, Z. H., Bin, D. Z., He, Z., & Wei, Z.W. (2016). Enhanced superconducting properties in MOD-YBCO thick films with  $\text{CeO}_2$  interlayer. *Acta Physica Sinica*. 65, 097401.

**Copyrights**

Copyright for this article is retained by the author(s), with first publication rights granted to the journal.

This is an open-access article distributed under the terms and conditions of the Creative Commons Attribution license (<http://creativecommons.org/licenses/by/4.0/>).